Spin-orbit interactions in an extended Tavis-Cummings system.

Alexander Tennant[1]

[1]University of Calgary

E-mail: aptennan@ucalgary.ca

David Feder

University of Calgary

E-mail: dfeder@ucalgary.ca

Abstract. Here we study a two and three atom Tavis-Cummings system in the ultra-cold regime where atoms interact with a spatially dependent coupling term. In this formalism, atoms are allowed to move within the cavity, and can therefore acquire momentum through their interactions with the cavity photons. We search for a specific set of cavity parameters that will allow us to realize a degeneracy in the lowest energy states of the system between states with different atomic momenta to possibly realize spin-orbit interactions within the cavity. As well, we search for interesting superposition states which may also indicate spin-orbit interactions. Using numerical methods in order to solve the system exactly, we find that in the case of very slow Rabi-oscillations and weak negative detuning that a degenerate low energy state is theoretically possible under very tightly controlled parameters. Relaxing the conditions yields interesting superposition states of spin and momentum, possibly indicating the presence of spontaneous spin-orbit interactions in cavity quantum electrodynamics.

1. Introduction

Cavity quantum electrodynamics (QED) offers a unique perspective with which one can model the interactions between the electric field and an atom trapped in a resonant cavity. In general, cavity QED systems are extremely complex and the even the simplest cases involving a single atom are not analytically tractable without making numerous approximations. One of the most famous toy models of a single atom interacting with a single electric field mode within a perfect cavity is known as the Jaynes-Cummings model [1, 2]. This model considers a stationary two-level atom interacting with an electric field mode which is nearly on resonance with the atomic transition frequency, or the frequency at which the atom will absorb a photon and under-go a spin-transition into its excited state. Another such toy model is the Tavis-Cummings [3, 4] model which considers the same type of system with multiple atoms trapped within the cavity.

However, new experiments with multiple atoms at ultra-cold temperatures [5, 9] find that these toy models are inadequate in their treatment of the atom as at rest. At such temperatures, the kinetic energy and spatial dependence of solutions can no longer be ignored as at these temperatures, the atoms kinetic energy will be noticeably affected by its interactions with the field. This study aims to understand these system at low temperatures, as well as to identify any interesting spin-orbit interactions occurring in the lowest energy states of a system containing multiple atoms, as the lowest energy states are where spin and momentum are tied directly; a pure spin-orbit interaction. In other words, the purpose of this investigation is to identify under what circumstances degeneracy can be obtained from modifying interactions between the electronic state and momentum of the atoms in the cavity. These relationships are currently of great interest as spin orbit interactions can result in exotic new states known as "topological insulators" [6], or a surface that has a conductive surface and an insulating interior.

This document will begin first by outlining the relevant back-ground of the simplified models that currently exist, as well as some of the solutions to problems that have already been solved in order to show that the formalism is being solved and applied correctly. We will first outline certain key aspects of the Jaynes-Cummings model relevant to this study, as well as the extension to model the dynamics of a single ultra-cold two-level atom moving through the standing wave optical potential due to the cavity. Once this is done, we will outline the basics of a multi-atom Tavis-Cummings model, at which point we will transition directly into the case of interest in this document - the dynamics of a two and three-atom system moving through a standing wave potential. The dynamics produce an energy band structure and we shall explore a few interesting "band crossings" in that section in order to probe for spin-orbit interactions. Finally, we shall move into the investigation of cavity parameters at which a degenerate energy system can be found between different excitation – analogous to spin – states of those atoms.

1.1. Jaynes-Cummings Model

The ideal starting point of this discussion is to introduce one of the few analytically solvable models in cavity quantum electrodynamics (QED): the Jaynes-Cummings (JC) model [1, 2]. The JC model describes the interactions between a single stationary two-level atom and an electric field mode trapped within a lossless resonant cavity. In order to realize an analytically solvable model several simplifying assumptions are made, such as the atoms only ever absorb or emit into the cavity mode, and the atom is considered at rest allowing the kinetic energy terms to be neglected. Under these assumptions, the JC Hamiltonian reads under the rotating wave approximation [7]:

$$\hat{H}_{JC} = \hbar\omega a^\dagger a + \frac{\hbar\omega_a}{2}\sigma_z + \hbar g(x)(a^\dagger\sigma^- + a\sigma^+), \tag{1}$$

where ω is the frequency of the field mode, ω_a is the atomic-transition frequency $a^\dagger$ and a are the photon creation and annihilation operators respectively, σ_z is the Pauli-z

matrix, σ^- and σ^+ are the spin raising and lowering operators, and $g(x)$ is the atom-field coupling term. For a full list of these operator definitions, please see Appendix A.

It is also important to note that $g(x)$ is the term which dictates the rates of stimulated emission and absorption. This term is most generally given by [7]:

$$g(x) = \frac{g_0}{\hbar}\left(\vec{d}\cdot\vec{E}(x)\right), \tag{2}$$

where g_0 is the atom-field coupling strength, $\vec{d}$ is the dipole moment of the atom, and $\vec{E(x)}$ is the electric field in the cavity. In the most basic case, the JC model ignores the spatial-dependence of Equation (2) and it is taken as invariant throughout the cavity, that is: $g(x) = g_0$, constant for all x [7].

As will become clear shortly, to simplify the analysis of this system it is convenient to define the quantity [7]:

$$\hat{N} = a^\dagger a + \sigma_z, \tag{3}$$

which is known as the excitation number operator. Upon inserting this into (1), it now takes the much more convenient form:

$$\hat{H}_{JC} = \hbar\omega\hat{N} + \frac{\hbar\Delta}{2}\sigma_z + \hbar g_0(a^\dagger\sigma^- + a\sigma^+), \tag{4}$$

where the quantity $\Delta \equiv \omega_a - \omega$ is known as the cavity detuning, or the difference in the atomic-transition frequency and the frequency of the cavity-mode. Equation (3) has the convenient property that it commutes with the Hamiltonian (4), meaning it is a conserved quantity, or constant, and can be neglected for any subsequent calculations, as it will only result in an energy shift without affecting the underlying dynamics, this commutation relation can be seen in Appendix B. It is now convenient to define the Rabi-frequency of this system, which is given by [7]:

$$\Omega = \sqrt{g^2(x)(n+1) + \Delta^2}, \tag{5}$$

which describes how often the atom transitions between the ground and excited states.

The Hamiltonian (4) has only two basis states: $|g, n\rangle$ and $|e, n-1\rangle$, where n is the photon number and g and e represent the atom in its ground and excited states respectively. Together with these states, Equation (4) defines a Hamiltonian matrix which consists of 2×2 blocks, which are block-diagonal in n:

$$\hat{H}_{JC} = \hbar\begin{pmatrix} +\frac{\Delta}{2} & g_0\sqrt{n} \\ g_0\sqrt{n} & -\frac{\Delta}{2} \end{pmatrix}, \tag{6}$$

this then defines the eigen-energies for a given block as:

$$E_n = \pm\hbar\sqrt{\frac{\Delta^2}{4} + (g_0)^2 n}. \tag{7}$$

It is then rather straightforward to solve this Hamiltonian with standard techniques of matrix exponentiation to solve for the time evolution of this system. This discussion, although of interest in many applications, is neglected for the purposes of this investigation as the time-dependence of this model is not of interest in this work.

1.2. Jaynes-Cummings Model With Quantized Motion

The standard JC model had great success in early cavity QED experiments where the atom was, quite literally, dropped into the cavity where it can then interact with the field until it eventually makes its way out of the cavity [8]. In experiments such as this, any changes to the momentum of the atom from its interactions with the field are negligible, and the Hamiltonian (4) describes systems such as this with surprising accuracy. However in new experiments with ultra-cold atoms interacting with highly confining trap potentials [9, 10] the kinetic energy then becomes comparable to that of the atomic-transition of the Hamiltonian. In these new experiments, the effects of the changes in momentum that atom under goes as it interacts with the electric field of the cavity can no longer be neglected. This means that the spatial dependence of Equation (2) can no longer be ignored.

Consider a boxed shaped cavity of length $L >> \lambda$ where λ is the wavelength of the photons within the cavity, such that the atom does not interact with the edges of the cavity. Under these boundary conditions the atom-field coupling term Equation (2) takes the form of a standing wave potential [7, 10, 11]:

$$g(x) = g_0 \cos(qx), \tag{8}$$

where $q = \frac{2\pi}{\lambda}$ is the wave number of the electric field mode. We also now must consider the atomic momentum states $|k\rangle$ where k is known as the atomic wave-vector or quasi-momentum [7, 10, 11]. In a box potential, these momentum eigenstates take the form of plane waves:

$$|k\rangle = \frac{1}{\sqrt{L}} e^{\frac{ikx}{L}}, \tag{9}$$

where i is the imaginary unit. The quasi momentum k can then take values in the range $-q \leq k < q$ [7, 10, 11]. The range $[-q, q)$ then defines the first Brillouin zone. If we assume that the atom in the cavity only interacts with the electric field along a single axis in the cavity, then we have the following Hamiltonian describing this new spatially dependant system [7, 10, 11]:

$$\hat{H}_{JC'} = \frac{\hat{P}^2}{2M} + \hbar\omega\hat{N} + \frac{\hbar\Delta}{2}\sigma_z + \hbar g_0 \cos(qx)(a^\dagger\sigma^- + a\sigma^+), \tag{10}$$

where $\hat{P}$ is the momentum operator and M is the mass of the atom. The Hamiltonian (10) and the excitation number operator Equation (4) preserve the commutation relation seen previously, and it is again sufficient to only consider the Hamiltonian:

$$\hat{H}_{JC'} = \frac{\hat{P}^2}{2M} + \frac{\hbar\Delta}{2}\sigma_z + \hbar g_0 \cos(qx)(a^\dagger\sigma^- + a\sigma^+), \tag{11}$$

The Hamiltonian (11) possesses some important symmetries which which should be considered. Most importantly is its invariance over all translations which satisfy the following [10, 11]:

$$T_1 = e^{i\lambda p}, \quad T_2 = \sigma_z e^{i\frac{\lambda}{2}p}, \tag{12}$$

where p is the momentum of the atom within the cavity. The first symmetry arises as a result of the cosine term describing the standing wave field mode, as this term is identical over all integer multiples of the wavelength λ. The second symmetry is not quite as obvious as it results from the fact that every time the momentum of the atom is changed by the field, the electronic state of the atom also changes either by absorbing or emitting a photon. This means that the atom has to undergo two translations before returning to its original electronic state. It is for this reason that we see periodicity between $[-q, q)$, rather than $[-\frac{q}{2}, \frac{q}{2})$, traditional of the Brillouin zone in phonon lattices [11].

With the addition of the kinetic energy terms, the Hamiltonian (11) no longer has the simple block diagonal form of Equation (4), rather it forms a tri-diagonal matrix which in general cannot be solved analytically [11, 12, 13]. In order to construct this new matrix, it is useful to note that:

$$\begin{aligned} 2\cos(qx)|k\rangle &= (e^{iqx} + e^{-iqx})e^{ikx} \\ &= e^{ix(k+q)} + e^{ix(k-q)} \\ &= |k+q\rangle + |k-q\rangle, \end{aligned} \tag{13}$$

as well as the new basis set which is defined by the following if the atom is initially in the ground state $|g\rangle$ [7, 10, 11] :

$$|\Psi(k)\rangle = \begin{cases} |k+mq, g, n\rangle & m \text{ even} \\ |k+mq, e, n-1\rangle & m \text{ odd}, \end{cases} \tag{14}$$

where m spans all integers and is the number of "momentum kicks" the atom has received from its interactions with the electric field. In this analysis it is always assumed that the atom is initially in the ground state, which defines the only zero-momentum state as $|0, g, n\rangle$. In the case where the atom is initially in $|e\rangle$, this simply redefines the zero momentum state which is equivalent to shifting to the second Brillouin zone.

In order to numerically solve Equation (11) the number of momentum kicks must be truncated at some dimension, in doing so the highest energy bands are subject to very serious truncation errors but if the matrix is large enough, the lowest energy bands should be nearly exact. For such a simulation, it is necessary to remove the units from this Hamiltonian by defining a new length scale. This is often done in terms of photon recoil energy ϵ [7, 10, 11], under this energy scale Equation (10) then takes the form:

$$\frac{\hat{H}_{JC}}{\epsilon} = -\frac{\partial^2}{\partial \tilde{x}^2} + \alpha\hat{N} + \frac{\tilde{\Delta}}{2}\sigma_z + \tilde{g}\cos(\tilde{x})(a^\dagger\sigma^- + a\sigma^+), \tag{15}$$

where

$$\begin{array}{lll} \epsilon \equiv \frac{\hbar^2 q^2}{2M}, & \alpha \equiv \frac{2M\omega}{\hbar q^2}, & \tilde{\Delta} \equiv \frac{2M\Delta}{\hbar q^2} \\ \tilde{g} \equiv \frac{2Mg_0}{\hbar q^2}, & \tilde{x} \equiv qx, & q \equiv 1 \\ \tilde{k} \equiv \frac{k}{q}, & & \end{array} \tag{16}$$

When Equation (11) is scaled in this way, it defines a tridiagonal matrix of the form:

$$\frac{\hat{H}_{JC}}{\epsilon} = \sum_{i=-p}^{p}\sum_{j=-p}^{p}\left[\left((\tilde{k}+j)^2 + \begin{cases} \frac{\tilde{\Delta}}{2} & j \text{ even} \\ -\frac{\tilde{\Delta}}{2} & j \text{ odd} \end{cases}\right)\delta_{m,n} + \sqrt{n}\tilde{g}(\delta_{i,j+1} + \delta_{i,j-1})\right], \tag{17}$$

where p is the maximum number of momentum "kicks". Upon solving this matrix numerically, subject to the initial state of $|0, g, n\rangle$, the band structure seen in Figure (1) is obtained. From Figure (1), it is clear that the detuning has the most dramatic

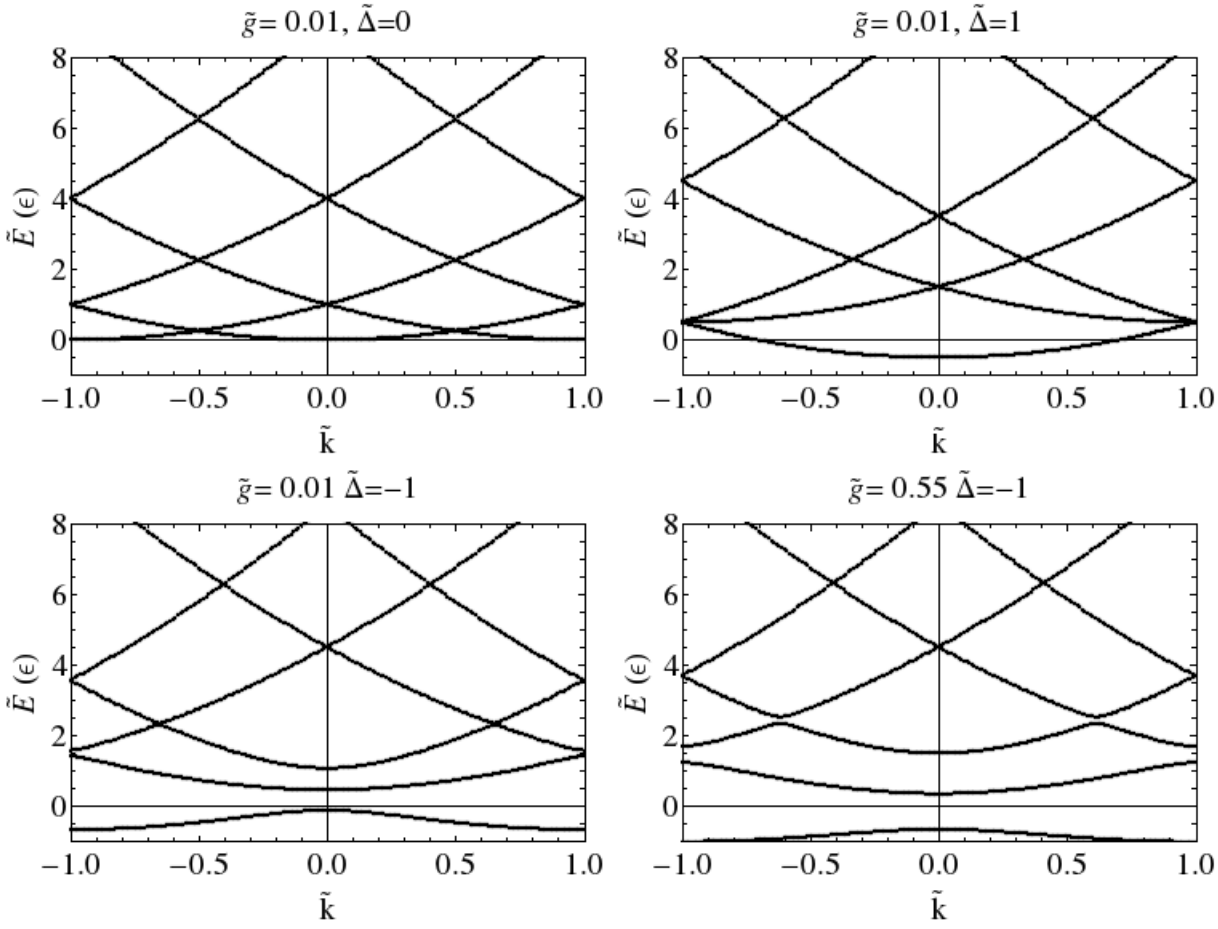

Figure 1. The Energy band structure of Equation (17) at various cavity detuning and atomic-transition strength. The key feature of these structures is when the energy band approaches the edge of the Brillouin zone and is then reflected back, the atom within the cavity both changed electronic state, as well as momentum.

and pronounced effect on the lowest few energy bands. This results from the fact that the higher energy bands have a larger contribution from the momentum of the atoms, which are significant enough to nullify the major effects of the detuning.

1.3. Tavis-Cummings Model

The Tavis-Cummings (TC) [3, 4] model is simply a generalization of the JC model which is able accommodate μ neutral identical stationary atoms interacting with a single cavity with an electric field mode. With generalized excitation number operator [14]:

$$\hat{N} = a^{\dagger}a + \sum_{i=1}^{\mu} \frac{\sigma_z^i}{2} \tag{18}$$

the TC Hamiltonian takes the following form under the rotating wave approximation:

$$\hat{H}(x_1, x_2, ..., x_\mu)_{TC} = \hbar\omega\hat{N} + \hbar\sum_{i=1}^{\mu}\left[g(x_i)(a^\dagger\sigma_i^- + a\sigma_i^+) + \frac{\Delta}{2}\sigma_{z_i}\right] \tag{19}$$

where $g(x_i)$ is identical in form to Equation (1), and μ is the number of atoms in the cavity. This Hamiltonian behaves in much the same way as Equation (1), except its blocks are of size 2^μ due to the additional electronic states from the other atoms. The main focus of this study is an extended TC Hamiltonian to account for the kinetic energy of each atom in the system as they undergo translational motion. In a box-shaped cavity with μ identical atoms under the same assumptions as Equation (10) as well as the assumption that the atoms will never collide with one another, the Hamiltonian takes a very similar form to that of an extended Dicke-Model [15]:

$$\begin{aligned}\hat{H}(x_1, x_2, .., x_\mu) = \hbar\omega\hat{N} + \sum_{i=1}^{\mu}\left(\frac{\hat{P}_i^2}{2M} + \frac{\hbar\Delta}{2}\sigma_{z_i}\right) \\ + 2g_0\sum_{i=1}^{\mu}\cos(qx_i)(a^\dagger\sigma_i^- + a\sigma_i^+).\end{aligned} \tag{20}$$

This Hamiltonian is invariant over the translations described in Equation (12), and in the two-atom case we have the following basis states for a given number of photons $n \geq 2$, such that the double excited states are accessible, by extending the states described in Equation (14), and assuming the initial state $|g, g, n\rangle$:

$$|\Psi(k_1, k_2)\rangle = \begin{cases} |k_1 + m_1 q, k_2 + m_2 q, n\rangle|g, g\rangle & m_1, m_2 \text{ even} \\ |k_1 + m_1 q, k_2 + m_2 q, n-1\rangle|e, g\rangle & m_1 \text{ odd}, m_2 \text{ even} \\ |k_1 + m_1 q, k_2 + m_2 q, n-1\rangle|g, e\rangle & m_1 \text{ even}, m_2 \text{ odd} \\ |k_1 + m_1 q, k_2 + m_2 q, n-2\rangle|e, e\rangle & m_1, m_2 \text{ odd}. \end{cases} \tag{21}$$

Once again, in general, Equation (20) is not analytically solvable, and must be solved numerically in order to observe an energy band structure similar to that of Figure (1). For such analysis, it is once again convenient to define the following unit less Hamiltonian, which is again scaled in terms of the photon recoil energy (16):

$$\begin{aligned}\frac{\hat{H}_{TC}(x_1, x_2)}{\epsilon} = \tilde{H} = \alpha\hat{N} + \sum_{i=1}^{2}\left(-\frac{\partial^2}{\partial\tilde{x}_i^2} + \frac{\tilde{\Delta}}{2}\sigma_{z_i}\right) \\ + 2\tilde{g}\sum_{i=1}^{2}\cos(\tilde{x}_i)(a^\dagger\sigma_i^- + a\sigma_i^+).\end{aligned} \tag{22}$$

Similarly to the JC model, the excitation number $\hat{N}$ commutes with the Hamiltonian, meaning that it is a conserved quantity and it is sufficient to consider only:

$$\tilde{H} = \sum_{i=1}^{2}\left(-\frac{\partial^2}{\partial\tilde{x}_i^2} + \frac{\tilde{\Delta}}{2}\sigma_{z_i}\right) + 2\tilde{g}\sum_{i=1}^{2}\cos(\tilde{x}_i)(a^\dagger\sigma_i^- + a\sigma_i^+). \tag{23}$$

Where the Hamiltonian (23) is somewhat more intricate in form than the JC version, Equation (17). Rather than defining a tridiagonal matrix, Equation (23) now

defines a matrix which has two off-diagonal elements for each atom (one element for absorption/emission in either direction of the cavity). An energy band structure, though still of interest, becomes more difficult to visualize as one now has to consider the momentum of all atoms involved. In the two-atom case, this means we now have two-dimensional momentum "planes" instead of the simple band structure seen in Figure (1).

2. Band Structure of the Two-Atom Tavis-Cummings Hamiltonian

Using standard numerical techniques, the two-atom case of Equation (22) can easily be solved for numerous values of the scaled detuning $\tilde{\Delta}$. In order to observe the complete structure, it is important that we have at least two photons in order that both atoms may be excited at the same time. We shall begin our focus on the energy band structure of Equation (22) and its similarities to Equation (17). In order to get a clear picture of the three-dimensional nature of the "band" structure of the two atom case, the most appropriate starting point is detailed look at the "ground plane" of the scaled Hamiltonian (22) in Figure (2).

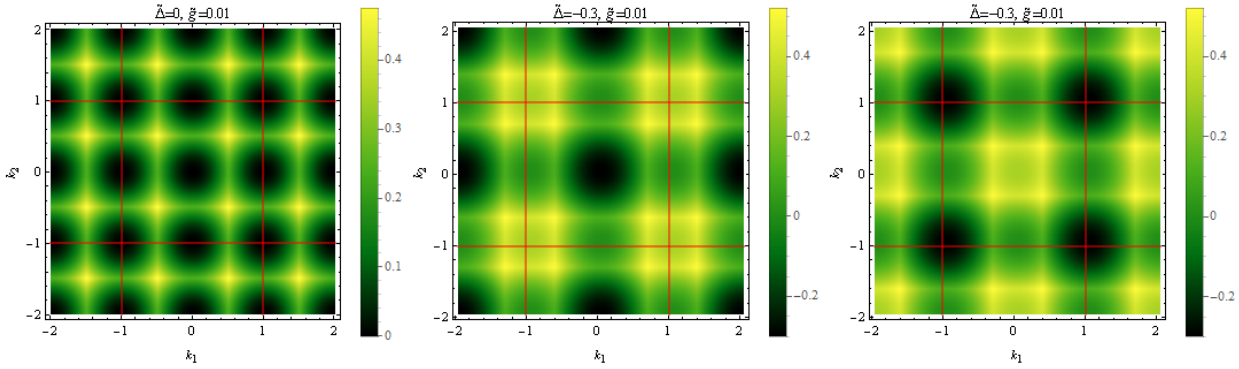

Figure 2. The lowest energy band at various detunings. Each axis is the scaled momentum of one atom, and the gradient represents the energy in terms of ϵ. The red lines traced over the plot represent the first Brillouin zone of $[-q, q)$. The first image is the structure obtained where the field is exactly on resonance with the atomic-transition frequency, or $\tilde{\Delta} = 0$. The second image displays the case of positive cavity detuning, and the third displays the case of negative cavity detuning. This structure is analogous to that of a phonon lattice, as the atoms can jump between "holes" as the atom's interact with the electric field.

From Figure (2), it is clear that even a small change in the detuning $\tilde{\Delta}$ can have a profound effect on the form of the lowest energy state of Equation (22). The center "hole" at the cases of small cavity detuning seen above is primarily composed of both atoms in the ground state with zero momentum. Likewise, the edges of the Brillouin zone are where one atom has interacted with the field to have $k \pm q$ of momentum, and the corners are where both atoms have transitioned into the excited state, each gaining $\pm q$ of momentum. With this three dimensional picture in mind, the band structure is

available in Figure (3) where we can observe "slices" of the three dimensional problem.

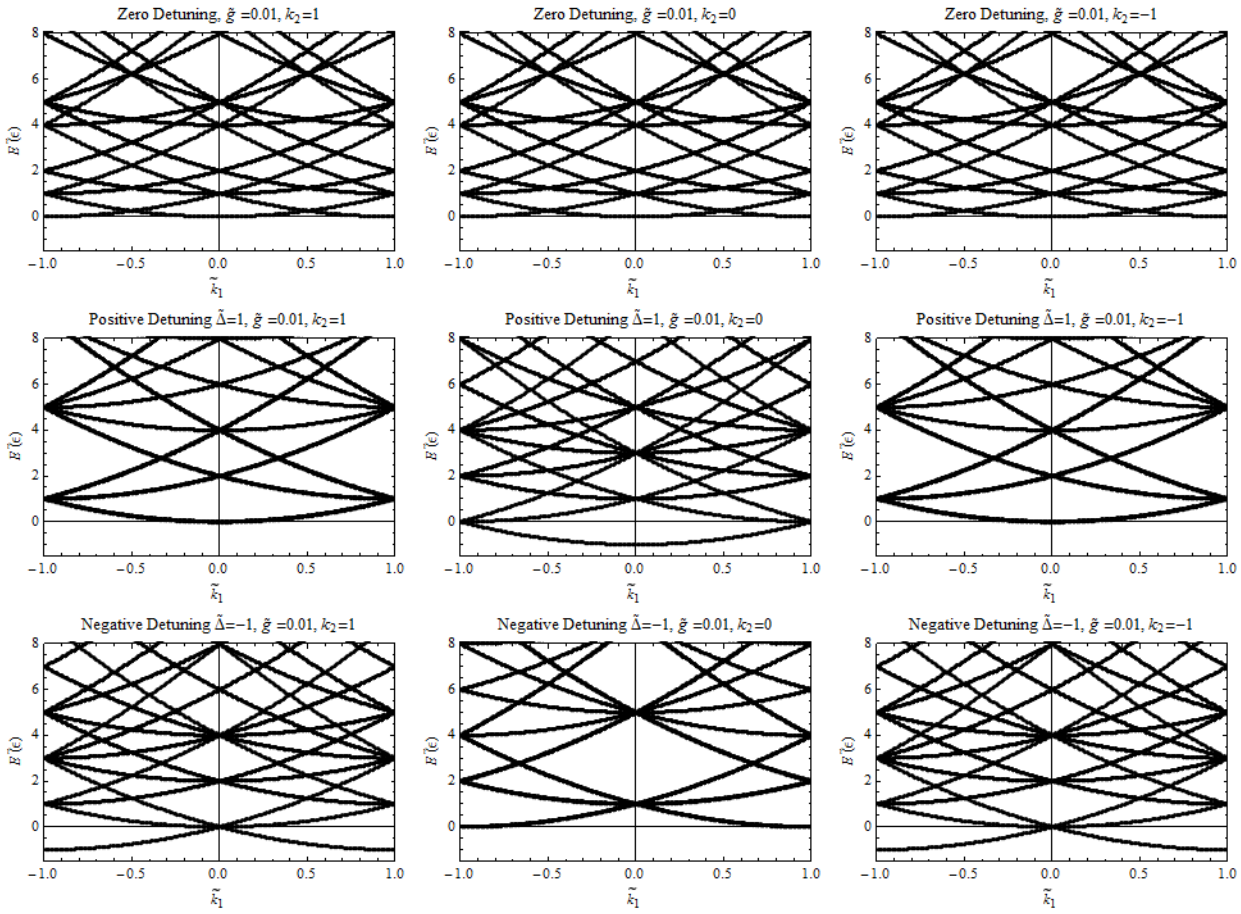

Figure 3. Here we see the bands structure of equation (23) at various detunings and momentum of the second atom. All plots subject to the initial condition $|0, 0, g, g, n\rangle$.

These plots in Figure (3) are shown within the first Brillouin zone of $[-q, q)$. Similarly to the band structure observed in Figure (1), the lowest energy bands of the two atom TC system are most dramatically affected by the detuning parameter $\tilde{\Delta}$. Pay particular notice to the band lowest energy bands in the negative detuning case, as this feature will become the focus of this paper in the coming sections.

2.1. Superposition of the ground state - Avoided Band Crossings.

In the previous subsection, we introduced the band structure of the scaled Hamiltonian (23), for the sake of completeness, we now explore this structure in finer detail than that seen in Figure (3). Below in Figure (4), we present a significantly closer looks at the negative detuning case, as well as included a case with large $\tilde{g}$ which increases the separation between bands:

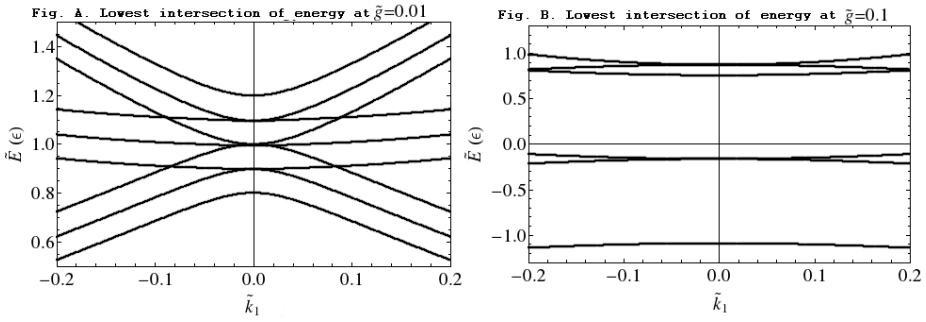

Figure 4. The first image seen in Fig. A. is a highly magnified feature of the lowest energy bands as seen in Figure (3), and the second image, Fig. B., is the same feature with $\tilde{g}$ taken to be 10 times larger. Both images are shown with $\tilde{\Delta} = -1.005$ and $\tilde{k}_2 = 0$.

At this scale, it is clear that while some degeneracies do exist between certain bands in the energy structure, the apparent total degeneracy seen in Figure (3) is actually comprised of a series of avoided crossings at finer scales. For a detailed investigation into the degeneracies, please refer to the next section. Our interest here is in the states that compose the non-degenerate lowest energy band at the point $\tilde{k}_1 = 0$ in Figure (4) in both the small and large $\tilde{g}$ cases, as if the atoms in the cavity are bosons, at low temperature this will be the only state occupied. As this energy state approaches the crossing, it is comprised mainly of a very few states - for example at $\tilde{k}_1 = 0.2$, it is easy to find numerically that the lowest band is comprised mostly of the following:

$$|\Psi(\tilde{k} = 0.2)\rangle = a|-q, -q, e, e, n-2\rangle + b|-q, 0, e, g, n-1\rangle + a|-q, q, e, e, n-2\rangle, \quad (24)$$

where $a < b$ and negligible contributions from higher energy states have been excluded. Likewise, its sister band at $\tilde{k}_1 = -0.2$ in Fig. A of Figure (4) is comprised by states identical to that of Equation (24), except the "second" atom is excited instead. The same is true in the large atom-field coupling case also shown in Figure (4), except at this scale this relationship is less obvious.

At the avoided crossing, the states are comprised of potentially interesting superpositions of many states. In atom optics, these avoided crossings along the center of the Brillouin zone are known as Bragg resonances [11, 16], which correspond to avoided crossings between two identical electronic states with opposite transverse momenta. The states that compose the ground state here are of interest as an equal superposition of the lowest energy states contributing to the lowest energy band could be indicative of a strong spin-orbit interaction. In the case of the lowest avoided crossing of Figure (4) in the weak atom-field coupling (and therefore low Rabi-frequency) case, we find using a numerical approach that the lowest energy state at the center Bragg resonance is:

$$\begin{aligned} |\Phi(\tilde{k}_1 = 0, \tilde{g} = 0.01)\rangle = \; & 0.353\{|-q, 0, e, g, n-1\rangle + |q, 0, e, g, n-1\rangle \\ & +|0, -q, g, e, n-1\rangle + |0, q, g, e, n-1\rangle\} \\ & -0.256\{|q, q, e, e, n-2\rangle + |q, -q, g, g, n-2\rangle \\ & +|-q, q, e, e, n-2\rangle + |-q, -q, e, e, n-2\rangle\} \\ & -0.487|0, 0, g, g, n\rangle \end{aligned} \quad (25)$$

Likewise for the Bragg resonance with stronger atom-field coupling:

$$\begin{aligned}|\Phi(\tilde{k}_1 = 0, \tilde{g} = 0.1)\rangle = \quad & 0.350\{|-q,0,e,g,n-1\rangle + |q,0,e,g,n-1\rangle \\ & +|0,-q,g,e,n-1\rangle + |0,q,g,e,n-1\rangle\} \\ & -0.259\{|q,q,e,e,n-2\rangle + |q,-q,g,g,n-2\rangle \\ & +|-q,q,e,e,n-2\rangle + |-q,-q,e,e,n-2\rangle\} \\ & -0.472|0,0,g,g,n\rangle\end{aligned} \quad .(26)$$

Where we have truncated negligible contributions from higher energy states. From Equations (25) and (26), it is clear that we are most probable to measure a singly excited state with momentum, with an approximately equal chance of measuring a state with no momentum in the double ground state, and a doubly excited state. The convenience of this result is in that this superposition is not heavily dependent on the Rabi-frequency, which is ideal as in practice the Rabi-frequency is difficult to control [20, 21].

This result has interesting implications - in actual experiment constraints on the coupling strength and Rabi-frequency do not necessarily have to be iron-clad. The superposition of Equations (25) and (26) can be observed at a wide range of coupling strength and Rabi-frequencies, and cavity detuning with minimal affect on the overall probability of observing each state. There may be a great deal of interest in this superposition, as measurement of the ground state at the Bragg resonance has a multitude of possible states all with different different momenta. While these energies are in no way degenerate, we see that the ground state is a super position of the lowest momentum states which may be a result of a strong spin-orbit interaction, as it may be possible to observe states with different transverse momenta and spin occupying the same energy.

3. The Search For Degeneracy in the Lowest Energy States.

3.1. Analytical Approximation of the Two-Atom Case

It is appropriate to first introduce some approximate analytical solutions in order to have some intuition into the results of our numerical simulations in the next section. Using the Hamiltonian (23), if we treat $\tilde{g}$ as a small perturbation, non-degenerate perturbation theory provides an appropriate treatment to understand the weak-coupling regime analytically. This is the case because as Figure (3) and Figure (4) suggest, degeneracies only arise with very specific restraints as a large atom-field coupling term cause bands to repel. These equations should describe all non-degenerate parameters, and where they fail should allow us to gain some insight into where degeneracies can be observed.

To begin, let's look at the form of Equation (23)

$$\tilde{H} = \underbrace{\sum_{i=1}^{2} -\frac{\partial^2}{\partial \tilde{x}_i^{\,2}} + \sum_{i=1}^{2} \frac{\tilde{\Delta}}{2}\sigma_z^i}_{\text{Diagonal Elements}} + \overbrace{\tilde{g}\sum_{i=1}^{2}\left\{\cos(\tilde{x}_i)(a^\dagger\sigma^- + a\sigma^+)\right\}}^{\text{Off-Diagonal Elements}}, \tag{27}$$

using this Hamiltonian, it is straightforward to calculate the energy of an arbitrary ground state $|k_1, k_2, g, g, n\rangle$ to second order. We find that the diagonal contribution from the unperturbed Hamiltonian is:

$$E_0 = k_1^2 + k_2^2 - \tilde{\Delta}. \tag{28}$$

Now it is simply a matter of understanding which states can couple directly to $|k_1, k_2, g, g, n\rangle$. The states that can couple with this are $|k_1 \pm 1, k_2, e, g, n-1\rangle$ and $|k_1, k_2 \pm q, g, e, n-1\rangle$, or the singly excited states with an appropriate momentum to emit into $|k_1, k_2, g, g, n\rangle$. This leaves us with a total of four off-diagonal couplings. If we recall from Equation (16) that $q \equiv 1$, we have the following:

$$E_{g,g} = k_1^2 + k_2^2 - \tilde{\Delta} - \tilde{g}^2 n\left[\frac{1}{2k_1 + \tilde{\Delta} + 1} + \frac{1}{-2k_1 + \tilde{\Delta} + 1} + \frac{1}{2k_2 + \tilde{\Delta} + 1} + \frac{1}{-2k_2 + \tilde{\Delta} + 1}\right]. \tag{29}$$

It is also easy to show for the doubly excited electronic state $|e, e\rangle$ which couples with the singularly excited states, and by limiting the couplings to the first Brillouin zone we have:

$$E_{e,e} = (k_1 \pm 1)^2 + (k_2 \pm 1)^2 + \tilde{\Delta} + \frac{\tilde{g}^2(n-1)}{(k_1 \pm 1)^2 + \tilde{\Delta} - k_1} + \frac{\tilde{g}^2(n-1)}{(k_2 \pm 1)^2 + \tilde{\Delta} - k_2}, \tag{30}$$

and for a single excitation $|e, g\rangle$:

$$E_{e,g} = (k_1 \pm 1)^2 + k_2^2 + \frac{\tilde{g}^2 n}{(k_1 \pm 1)^2 + k_1 + \tilde{\Delta}} + \frac{\tilde{g}^2(n-1)}{k_2 - (k_2+1)^2 - \tilde{\Delta}} + \frac{\tilde{g}^2(n-1)}{k_2 - (k_2-1)^2 - \tilde{\Delta}}, \tag{31}$$

where we simply have to switch the indices's for the state $|g, e\rangle$. From the above equations, we see that for a given Brillouin zone, there is only a single $|g, g\rangle$ state, four $|e, e\rangle$ states, and two of each $|e, g\rangle$ and $|g, e\rangle$, all with different momentum.

From the form of Equations (29), (30) and (31), we see that these energies should appear linear as function of the detuning $\tilde{\Delta}$ with sufficiently small $\tilde{g}$. By taking the limit as $\tilde{g} \to 0$ we find that we should observe degeneracies between given states where:

$$\begin{aligned} E_{g,g} &= E_{e,g} \quad \Rightarrow -\tilde{\Delta} = 2k_1 + 1 \\ E_{g,g} &= E_{g,e} \quad \Rightarrow -\tilde{\Delta} = 2k_2 + 1 \\ E_{g,g} &= E_{e,e} \quad \Rightarrow \tilde{\Delta} = \pm k_1 + \pm k_2 + 1. \end{aligned} \tag{32}$$

Due to multiple degeneracies which can be observed in the band structure, there are a multitude of cases where these solutions will fail. Do to the nature of the problem degenerate perturbation theory will not, in general, offer us analytic solutions as degeneracy can be observed between up to all nine of the lowest energy states. Despite this, these equations should offer a reasonable guide as to where degeneracy can be observed in an exact numerical simulation, and be near exact in the small $\tilde{g}$ domain, far from any degeneracies.

3.2. Numerical Results

We shall first explore the regime that which is difficult to understand analytically with perturbation theory, in a high Rabi-frequency case where $\tilde{g}$ is a significant contribution to the total energy of the Hamiltonian. Solving the Hamiltonian a function of $\tilde{\Delta}$ for a given $\tilde{g}$, we obtain the following for both the two and three atom cases:

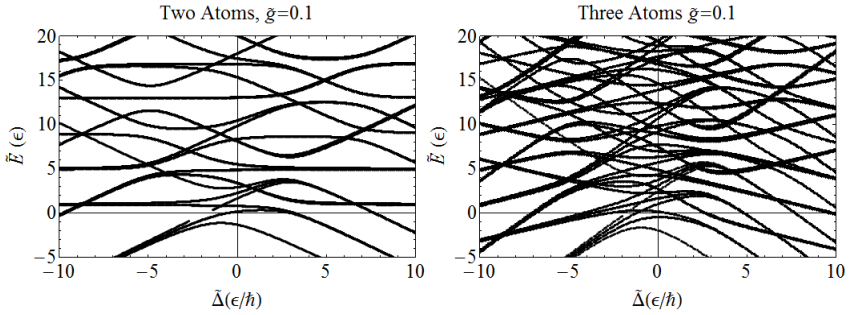

Figure 5. This figure shows the energy structure of the quantized motion TC Hamiltonian for two and three atoms as a function of the detuning $\tilde{\Delta}$ where the atom-feild coupling is large enough to have a significant impact on the total energy of the Hamiltonian.

From Figure (5), it is obvious that the lowest energy states will never exhibit any degeneracy between states with different momenta as a function of the detuning, except in the asymptotic limit as $\tilde{\Delta} \to \infty$. This fact is obvious from the form of the lowest energy level, where the ground-state curve approaches an asymptote at $\tilde{\Delta} \approx -1$. No curves ever cross each other with complete degeneracy until we reach higher energy states. Based on these figures, we now limit our search for degeneracy to the weak-coupling regime where $\tilde{g}$ is small, and our approximate analytic equations should describe the system with reasonable accuracy away from any degeneracies.

After diagonalizing the TC Hamiltonian (23) for both the two and three atom cases with weak coupling, we obtain the following:

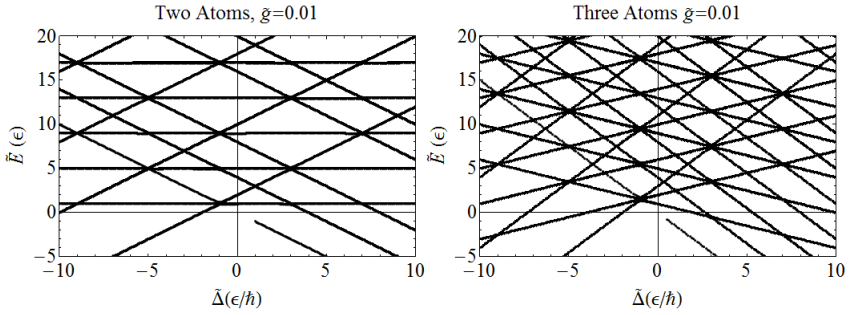

Figure 6. Using our solutions from the previous section, we find that away from the degenerate points the electronic states of $|g, g\rangle$, $|e, e\rangle$ and any combination of $|e, g, \rangle$ have a slope of -1, 1 and 0 respectively. In the three atom case, whose approximate forms can be seen in the appendix, electronic states $|g, g, g, \rangle$, $|e, e, e\rangle$ and any combination of $|e, g, g, \rangle$ and $|e, e, g\rangle$ have slopes of $-3/2$, $3/2$, $-1/2$ and $1/2$ respectively.

Figure (6) is a much more interesting figure. Upon close inspection of the lowest energy curves, we find that in both the two and three atom cases that there appears to be a low-energy degeneracy at approximately $\tilde{\Delta} = -1$. This feature is unsurprising if one is to recall the negative detuning case of Figure (3). At this scale, all energy levels appear to be completely degenerate, however a closer inspection is required in order to investigate this feature completely. Upon focusing on that feature, we obtain Figure (7).

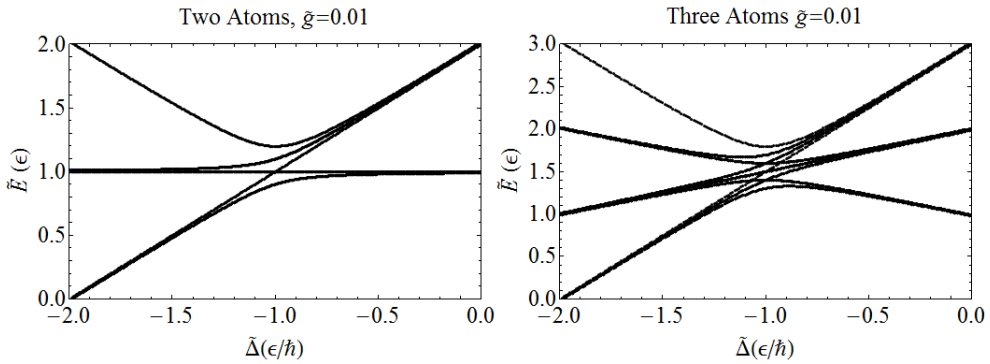

Figure 7. Here we see that there is a very clear and distinct intersection in energy of states with different momenta.

Figure (7) shows a very clear energy degeneracy for states with different momenta – and even more so in the three-atom case. In the two atom case, the intersection between the excited and the singularly excited case happens at $\tilde{\Delta}$ = -1.005. This corresponds to the following eigenvectors, written in terms of our original basis (21):

$$\begin{aligned} |\Psi_1\rangle = \quad & 0.147\{|q,0,e,g,n-1\rangle - |-q,0,e,g,n-1\rangle\} \\ & -0.486\{|0,q,g,e,n-1\rangle - |0,-q,g,e,n-1\rangle\} \\ & -0.232\{|q,q,e,e,n-2\rangle - |-q,-q,e,e,n-2\rangle\} \\ & -0.434\{|-q,q,e,e,n-2\rangle - |q,-q,e,e,n-2\rangle\}, \end{aligned} \tag{33}$$

and

$$\begin{aligned} |\Psi_2\rangle = \quad & 0.486\{|q,0,e,g,n-1\rangle - |-q,0,e,g,n-1\rangle\} \\ & -0.147\{|0,q,g,e,n-1\rangle - |0,-q,g,e,n-1\rangle\} \\ & -0.434\{|q,q,e,e,n-2\rangle - |-q,q,e,e,n-2\rangle\} \\ & -0.232\{|q,-q,e,e,n-2\rangle - |-q,-q,e,e,n-2\rangle\}, \end{aligned} \tag{34}$$

where we have truncated negligible contributions from higher energy states.

From Equations (33) and (34), we see that a measurement of the degenerate energy has approximately a 50% chance of having two quanta of momentum, or a state with only a single quanta of momentum with each state occupying that energy. This implies that there is a very interesting spin-orbit interaction happening, as there is a possibility that measurement could yield two atoms with different transverse momenta and opposite spins with *identical* energies. The same type of degeneracy is observed in the three-atom case, except multiple degeneracies can be observed between the states that have

momenta. These multiple degeneracies between states with different atomic-momenta seem to suggest that this effect will be more easily observed in cavities which contain multiple atoms.

Of course, the question now arises as to how experimentally realizable this result is. If we assume that there are enough photons in the cavity such that each atom always has equal probability of excitation and that the Rabi-frequency is comparable to that of the standard TC model which does not consider transverse momenta, the Rabi-frequency of each atom is approximately given by [18]:

$$\Omega = \sqrt{ng^2 + \frac{\Delta^2}{4}}. \tag{35}$$

If we return to our scaled units of Equation (16), we find that at optical wavelengths with $\tilde{\Delta} = -1.005$ and $\tilde{g} = 0.01$ that the Rabi Frequency of this system is then:

$$\Omega \approx 2.5 \times 10^5 \text{ Hz}, \tag{36}$$

and at microwave wavelengths:

$$\Omega \approx 2500 \text{ Hz}, \tag{37}$$

both of these values are at the bottom end of current experimental technique [19, 21, 22, 22], but not far outside the realm of possibility. The primary challenge to over come is the minuscule requirement on cavity detuning, which is on the order of 50 KHz. In most experiment this is normally either exactly zero, or on the order of MHz [22, 23].

4. Conclusions and Outlook

Spin-orbit interactions are of interest in many applications in physics, one of the most notable applications is the exotic states of topological insulators [6, 17]. Normally, these systems are realized using ultra-cold atomic gases often using rare and expensive metals. In practice these states are difficult to realize without very careful experimental controls on a many body system. It is also often required to maintain high particle density and lattice structure in atomic gases, which adds challenges to maintaining the ultra-cold temperatures required for these systems [6, 17]. Due to these challenges, it is always of interest to discover novel ways of creating and observing these states experimentally.

These results seem to suggest the possibility of observing spin-orbit interactions between the electronic state of an atom, and its momentum in an ultra-cold cavity QED system, analogous to the topological insulators. However, experimental confirmation of these results could be quite difficult. Often, these experiments are done with heavy atoms such as cesium and rubidium. At optical wavelengths, the Rabi-frequencies and cavity detuning required to observe degenerate eigenstates are incredibly small by experimental standards and could be difficult to obtain. However, recent work has shown very low Rabi-Frequencies on the order of 3500 Hz [21] using cesium at microwave

wavelengths, but the main hurdle to overcome is the minuscule values required for atom-field detuning.

We have also shown that spin-orbit interactions can be observed in systems with more realistic atom-field coupling strength and cavity detuning more easily realized with current experimental techniques. These frequencies are approximately 10 times larger than that those required by the cases involving degeneracy, and exactly on resonance detuning. Depending on the photon number of the cavity, most Rabi-frequencies are on the order of 7-500 KHz [7, 19, 21, 22]. Under these conditions it could be possible to measure states with different spin and momentum occupying the ground state of the system at different times. While in these cases it is not, in general, possible to also measure degeneracy between the lowest energy states, it could still be possible to experimentally confirm a spin-orbit interactions which have become evident from the superposition of the ground state in this regime.

Despite the possible difficulties involved in an experimental realization, these results seem to suggest a novel was of observing states analogous to that of a topological insulator using a cavity QED approach, rather than an ultra-cold atomic gas. While this method has experimental challenges of its own, it may be of interest to study spin-orbit interactions with very few atoms rather than an entire lattice. Further work needs to be done to investigate if variations in parameters other than the detuning and coupling strength yield these strong spin orbit interactions, such as cavity size as well as type and number of atoms trapped within the cavity. Even so, these results suggest that in well controlled ultra-cold cavity QED systems, experimental realization of degeneracy in low energy states and the superposition of the ground state may be within reach of current experimental techniques.

References

[1] E.T. Jaynes, F.W. Cummings, 1963, *Comparison of Quantum and Semiclassical Radiation Theories with Application to the Beam Maser, Proc. IEEE* **51**,89.

[2] E.T. Jaynes, 1965, *Stimulated Emission of Radiation in a Single Mode, Phys. Rev. A.* **140**, 1051.

[3] M. Tavis, F.W. Cummings, 1968, *Exact Solution for an N-Molecule Radiation-Field Hamiltonian, Phys.Rev.* **170**, 379.

[4] M. Tavis, F.W. Cummings, 1969, *Approximate Solutions for an N-Molecule-Radiation-Field Hamiltonian, Phys. Rev* **188**, 692.

[5] F. Brennecke, T. Donner, S. Ritter, T. Bourdel, M. Kőhl, T. Esslinger, 2007, *Cavity QED with a Bose-Einstein condensate, Nature* **450**, 268.

[6] C. L. Kane, 2008, *Condensed matter: An insulator with a twist, Nature Phys.* **4**, 348.

[7] J. Larson, 2005, *Extended Jaynes-Cummings models in cavity QED, Doctoral Thesis.*

[8] D. E. Pritchard, A.D. Cronin, S. Gupta, D. A. Kokorowski, 2001 *Atom optics: Old ideas, current technology, and new results Ann. Phys. (Leipzing)* **10**, 35.

[9] I.B. Mekhov, C. Maschler, H. Ritsch, 2007, *Probing quantum phases of ultra cold atoms in optical lattices by transmission spectra in cavity quantum electrodynamics, Nat. Phys.* **3**, 319.

[10] J. Larson, J. Salo, S. Stenholm, 2005, *Effective mass in cavity QED, Phys. Rev A* **72**, 013813-1.

[11] M. Wilkens, E. Schumacher, P. Meystre, 1991, *Band theory of a common model of atom optics, Phys. Rev. A* **44**, 3130.

[12] A. Vaglica, 1995 *Jaynes-Cummings model with atomic position distribution, Phys. Rev. A* **52**, 2319.

[13] A.M. Herkommer, V.M. Akulin, W.P. Schleich, 1992, *Quantum Demolition Measurement of Photon Statistics by Atomic Beam Deflection, Phys. Rev. Lett.* **69**, 3298.

[14] N. M. Bogoliubov, R.K. Bullough, J Timonen, 1996, *Exact solution of generalized Tavis-Cummings models in quantum optics, J. Phys. A:Math Gen.* **29**, 6305.

[15] J. Larson, M. Lewenstein, 2009, *Dilute gas of ultracold two-level atoms inside a cavity: generalized Dicke model, New J. Phys.* **11**, 063027.

[16] S. Glasgow, P. Meystre, M. Wilkens, 1992, *Doppleron-catalyzed Bragg resonances in atom optics, Opt. Lett.* **17**, 1301

[17] M. Z. Hasan, C. L. Kane, 2010, *Colloquium: Topological Insulators, Rev. Of. Mod. Phys.* **82**, 3045.

[18] M. G. Kozerovskii, S.M. Chumakov, 1994, *Exactly solvable Dicke models and radiation dragging, J. of Rus. Laser Res.* **15**, 118.

[19] M. Reetz-Lamour,J. Deiglmayr, T. Amthor, M. Weidmeuller, 2008, *Rabi Oscillations between ground and Rydberg states and van der Waals blockade in a mesoscopic frozen Rydberg gas, New J. Phys.* **10**, 045026.

[20] M. Ebert, A. Gill, M. Gibbons, X. Zhang, M. Saffman, T. Walker, 2013, *Atomic Fock State Preparation Using Rydberg Blockade, arXiv:1310.7561v1.*

[21] M. Kinoshita, K. Shimaoka, K. Komiyama, 2008, *Rabi Frequency Measurement for Microwave Power Standard Using Double Resonance Spectrum, Prec. Electromag. Meas. Dig.* 1-4244-2399

[22] M.C. Fischer, K.W. Madison, Q. Niu, M .G. Raizen, 1998, *Observation of Rabi oscillations between Bloch bands in an optical potential, Phys. Rev. A* **58**, R2648

[23] D. Weiss, E. Riis, Y. Shevy, P. Jeffery, S. Chu. 1989, *Optical molasses and multilevel atoms: experiment, J. Opt. Soc. Am. B.* **6**, 2072.

Appendix A. States and Operators.

Here we define the set of operators used for this analysis. The most basic operators are those describing the ground and excited state. That is:

$$|e\rangle \equiv \begin{pmatrix} 1 \\ 0 \end{pmatrix}, \quad |g\rangle \equiv \begin{pmatrix} 0 \\ 1 \end{pmatrix}, \tag{A.1}$$

the vectors which describe the atom in the excited or in the ground state. The Pauli-z matrix is then defined as the following:

$$\sigma_z = \ |e\rangle\langle e| - |g\rangle\langle g| = \ \begin{pmatrix} 1 & 0 \\ 0 & -1 \end{pmatrix}, \tag{A.2}$$

which is the operator that tracks the excitations of the atoms in the cavity. The raising and lowering operators are then defined by:

$$\sigma^+ = |e\rangle\langle g| = \begin{pmatrix} 0 & 1 \\ 0 & 0 \end{pmatrix}, \quad \sigma^- = |g\rangle\langle e| = \begin{pmatrix} 0 & 0 \\ 1 & 0 \end{pmatrix}, \tag{A.3}$$

the photon creation an annihilation operators act on a number stater $|n\rangle$ such that:

$$a^\dagger|n\rangle = \sqrt{n+1}|n+1\rangle, \quad a|n\rangle = \sqrt{n}|n-1\rangle, \tag{A.4}$$

Finally, the kinetic energy operator acts on some momentum state $|k+q\rangle$ as

$$\frac{\hat{P}^2}{2M}|k+q\rangle = -\frac{\hbar^2}{2M}\frac{\partial^2}{\partial x^2}e^{i(k+q)x} = \frac{(k+q)^2\hbar^2}{2M}|k+q\rangle, \tag{A.5}$$

Appendix B. The Commutation of $\hat{N}$ and Hamiltonian

It is easy to show that with the excitation number operator

$$\hat{N} = a^\dagger a + \sum \frac{\sigma_z}{2}, \tag{B.1}$$

and the Hamiltonian

$$\tilde{H} = \alpha\hat{N} + \sum\left(-\frac{\partial^2}{\partial\tilde{x}_i^2} + \frac{\tilde{\Delta}}{2}\sigma_{z_i}\right) + 2\tilde{g}\sum\cos(\tilde{x}_i)(a^\dagger\sigma_i^- + a\sigma_i^+), \tag{B.2}$$

That these two terms commute. That is:

$$\left[\hat{N}, \hat{H}\right] = 0, \tag{B.3}$$

For simplicity, it is important to note that most of these operators are applied to different product spaces, and the only term that therefore does not trivially commute is:

$$\begin{aligned} \left[\hat{N}, a^\dagger\sigma^-\right] &= \left[a^\dagger a, a^\dagger\sigma^-\right] + \left[\sigma_z, a^\dagger\sigma^-\right] \\ &= a^\dagger\sigma^- - \sigma^- a^\dagger = 0 \\ \left[\hat{N}, a\sigma^+\right] &= \left[a^\dagger a, a\sigma^+\right] + \left[\sigma_z, a\sigma^+\right] \\ &= a\sigma^+ - \sigma^+ a = 0, \end{aligned} \tag{B.4}$$

where the cosine term of the Hamiltonian has been neglected as it affects a different product space, and therefore commutes trivially.

Appendix C. Approximate solutions for the 3-atom case

In order to understand Figure (6), we need only to approximate the Hamiltonian (23) (for the three atom case) to first order. In doing so, we find the following:

$$E_{g,g,g} = k_1^2 + k_2^2 + k_3^2 - \frac{3\tilde{\Delta}}{2} \tag{C.1}$$

$$E_{e,e,e} = (k_1 \pm 1)^2 + (k_2 \pm 1)^2 + (k_3 \pm 1)^2 + \frac{3\tilde{\Delta}}{2} \tag{C.2}$$

$$E_{e,g,g} = (k_1 \pm 1)^2 + k_2^2 + k_3^2 - \frac{\tilde{\Delta}}{2} \tag{C.3}$$

where one simply has to switch indices's for the $|g,e,g\rangle$ and $|g,g,e\rangle$ states. We also have:

$$E_{e,e,g} = (k_1 \pm 1)^2 + (k_2 \pm 1)^2 + k_3^2 + \frac{\tilde{\Delta}}{2} \tag{C.4}$$

Where again, we need only switch indices's for the states $|g,e,e\rangle$ and $|e,g,e\rangle$. These first order solutions are sufficient to understand the structure of figure (6). As well, we now see that the intercept at $\tilde{\Delta} = 0$ provides us with an idea of the total momentum of the state.

Appendix D. Mathematica Code

This is the code for the two-atom case. The single-atom and three-atom cases are similar in form, but modified to account for a different number of atoms. To avoid redundancy, they have been neglected from this appendix.

```
StateMaker[katom1_, katom2_, photons_, Q_] := (*This defines all the states*)
 Table[
  If[s1 == s2 == 1 && n ≥ 2 && OddQ[q] == True && OddQ[q2] == True,
   {1, Q*q, Q*q2, s1, s2, n - 2},
   If[s1 == s2 == 0 && EvenQ[q] == True && EvenQ[q2] == True,
    {1, Q*q, Q*q2, s1, s2, n},
    If[OddQ[q] == True && s1 == 1 && EvenQ[q2] == True && s2 == 0,
     {1, Q*q, Q*q2, s1, s2, n - 1},
     If[EvenQ[q] == True && s1 == 0 && OddQ[q2] == True && s2 == 1,
      {1, Q*q, Q*q2, s1, s2, n - 1},
      ## &[]
     ]
    ]
   ](*Vanishingfunction*)
  ],
  {q, -katom1, katom1}, {q2, -katom2, katom2}, {s1, 0, 1}, {s2, 0, 1}, {n, photons, photons}]
```

```
NOp[state_, A_] := {ReplacePart[state, 1 → A*state[[6]]]};
(*number operator and kinetic energy operator*)
Kin[state_, k1_, k2_, scale_] :=
  (*Resolves the kinetic energy terms of each atom*)
  {ReplacePart[state, 1 → scale (k1+ state[[2]])^2],
   ReplacePart[state, 1 → scale (k2 + state[[3]])^2]};
PaulZ[state_, A_] := (*PaulZ operator on given state*)
 {If[state[[5]] = 0,
   ReplacePart[state, 1 → -A/2 *state[[1]]],
   ReplacePart[state, 1 → A/2 *state[[1]]]],
  If[state[[4]] = 0,
   ReplacePart[state, 1 → -A/2 *state[[1]]],
   ReplacePart[state, 1 → A/2 *state[[1]]]]}
```

```
Emission[state_, g_, A_] := (* emission of a photon*)
  {
   If[
    state[[5]] = 1,
    ReplacePart[state, {5 → 0, 6 → state[[6]] + 1, 1 → g*A Sqrt[state[[6]] + 1]}],
    ## &[]],
   If[
    state[[4]] = 1,
    ReplacePart[state, {4 → 0, 6 → state[[6]] + 1, 1 → g* A Sqrt[state[[6]] + 1]}],
    {0, 0, 0, 0, 0, 0}]
   (*If[state[[4]]=state[[5]]=1,
    ReplacePart[state,{4→ 0,5→0,6→ state[[6]]+2,1→ state[[6]]+1}],
    ##&[]]*)
  };
Absorption[state_, g_, A_] := (*absorption of a photon*)
 {
  If[
   state[[5]] = 0 && state[[6]] > 0,
   ReplacePart[state, {5 → 1, 6 → state[[6]] - 1, 1 → g*A Sqrt[state[[6]]]}],
   ## &[]],
  If[
   state[[4]] = 0 && state[[6]] > 0,
   ReplacePart[state, {4 → 1, 6 → state[[6]] - 1, 1 → g*A Sqrt[state[[6]]]}],
   {0, 0, 0, 0, 0, 0}]
  (*If[state[[4]]=0 &&state[[5]]=0 && state[[6]]≥ 2,
   ReplacePart[state,{4→ 1,5→1,6→ state[[6]]-2,1→ state[[6]]}],
   ##&[]]*)}
```

```
FC[state_, Q_] := (*This function takes the emission and absorption
  stuff and changes the momentum states accordingly*)
 If[
  Length@state == 2,
  Flatten[Table[
    If[state[[i]] == {0, 0, 0, 0, 0, 0},
     {{0, 0, 0, 0, 0, 0}},
     {
      ReplacePart[state[[i]], j → (state[[i, j]] + Q)],
      ReplacePart[state[[i]], j → (state[[i, j]] - Q)]
     }
    ],
    {i, 1, 2}, {j, 2, 3}], 2],
  If[Length@state == 1 && state[[1]] ≠ {0, 0, 0, 0, 0, 0},
   Flatten[Table[
     {
      ReplacePart[state[[1]], i → (state[[1, i]] + Q)],
      ReplacePart[state[[1]], i → (state[[1, i]] - Q)]
     }, {i, 2, 3}], 1],
   {{0, 0, 0, 0, 0, 0}}]
 ]
```

```
ActOnState[state_, Q_, g_, A_, B_, C_, D_, k1_, k2_, scale_] := Block[
   {effect},
   effect = {};
   AppendTo[effect, Kin[state, k1, k2, scale]];
   AppendTo[effect, NOp[state, A]];
   AppendTo[effect, PaulZ[state, B]];
   AppendTo[effect, FC[Emission[state, g, C], Q]];
   AppendTo[effect, FC[Absorption[state, g, D], Q]];
   {effect}
  ];
(*Function to act the Hamiltonian on a given state and flatten it appropriately.*)
HState[state_, Q_, g_, A_, B_, c_, D_, k1_, k2_, scale_] :=
 Flatten[ActOnState[state, Q, g, A, B, c, D, k1, k2, scale], 2]
KCheck[act_, raw_] := (*Off diagonal terms*)
  If[raw[[2]] == act[[2]] && raw[[3]] == act[[3]],
   1,
   0];
(*Finds all non zero terms*)
IsItZero[raw_, act_] := Block[
  {total},
  total = {};
  Do[
   If[raw[[4]] == act[[i, 4]] && raw[[5]] == act[[i, 5]] && raw[[6]] == act[[i, 6]],
    AppendTo[total, act[[i, 1]] * KCheck[act[[i]], raw]],
    AppendTo[total, 0]],
   {i, 1, Length[act]}];
  total = Total[total];
  {total}
 ]
```

```
HamiltonianShmamiltonain[states_, Q_, g_, A_, B_, C_, D_, k1_, k2_, scale_] :=
  (*Make hamiltonian*)
  Table[
   Table[
    First@IsItZero[states[[i]], HState[states[[j]], Q, g, A, B, C, D, k1, k2, scale]]
    , {j, 1, Length[states]}
   ],
   {i, 1, Length[states]}
  ];
thing[k1_, k2_, scale_, states_, Q_, g_, A_, B_, C_, D_] :=
  (*Make Hamiltonain Numerical only*)
  N@HamiltonianShmamiltonain[states, Q, g, A, B, C, D, k1, k2, scale];
```

```
points = {};
plots = {};
Look = {{0, 0}, {2, 0}, {4, 6}, {10, 3}};
(*generate points for plots*)
Do[
  Do[
    {
     AppendTo[points,
      Partition[
       Riffle[
        Eigenvalues[Calculations /. {a → Look[[j, 1]], b → Look[[j, 2]], d → i, g → .01}]
        (*All this hocus pocus is just to make ordered psirs to plot*)
        , i]
       , 2]
     ]
    }
    , {i, -30, 30, .11}
   ]
   points = Map[Reverse, points, {2}];
  AppendTo[plots, ListPlot[Transpose@points,
    PlotMarkers → None,
    PlotStyle → Black,
    ImageSize → 500,
    Frame → True,
    FrameLabel → {"Δ̃(ϵ/ħ)", "Ẽ (ϵ)"},
    (*PlotRangePadding→ None,*)
    LabelStyle → Large,
    PlotLabel → Style[Row[Flatten[{{"k₁ =", Look[[j, 1]], " "}, {"k₂ =" , Look[[j, 2]]}}]], Large]
   ]];
  points = {};
  , {j, 1, 4}] // AbsoluteTiming
```